

FREQUENCY-AWARE MASKED AUTOENCODERS FOR MULTIMODAL PRETRAINING ON BIOSIGNALS

Ran Liu^{1,2*}, Ellen L. Zippi¹, Hadi Pouransari¹, Chris Sandino¹, Jingping Nie^{1,3*}
Hanlin Goh¹, Erdrin Azemi¹, Ali Moin¹
Apple¹, Georgia Institute of Technology², Columbia University³

ABSTRACT

Leveraging multimodal information from biosignals is vital for building a comprehensive representation of people’s physical and mental states. However, multimodal biosignals often exhibit substantial distributional shifts between pretraining and inference datasets, stemming from changes in task specification or variations in modality compositions. To achieve effective pretraining in the presence of potential distributional shifts, we propose a frequency-aware masked autoencoder (`bioFAME`) that learns to parameterize the representation of biosignals in the frequency space. `bioFAME` incorporates a frequency-aware transformer, which leverages a fixed-size Fourier-based operator for global token mixing, independent of the length and sampling rate of inputs. To maintain the frequency components within each input channel, we further employ a frequency-maintain pretraining strategy that performs masked autoencoding in the latent space. The resulting architecture effectively utilizes multimodal information during pretraining, and can be seamlessly adapted to diverse tasks and modalities at test time, regardless of input size and order. We evaluated our approach on a diverse set of transfer experiments on unimodal time series, achieving an average of $\uparrow 5.5\%$ improvement in classification accuracy over the previous state-of-the-art. Furthermore, we demonstrated that our architecture is robust in modality mismatch scenarios, including unpredicted modality dropout or substitution, proving its practical utility in real-world applications. Code will be available soon.

1 INTRODUCTION

Physical and mental states of an individual are manifested by a variety of physiological responses or *biosignals*. For example, electroencephalography (EEG) can decode human emotions by monitoring their brain activities (Liu et al., 2010), electromyography (EMG) can detect facial expressions such as smiling by recording muscle contractions (Canento et al., 2011), and a combination of these modalities can help decode a person’s affective states. The effective use of multimodal information can not only build better and more resilient representations of the human body and mental states (Bachmann et al., 2022; Smith & Gasser, 2005; De Sa & Ballard, 1998), but also help researchers understand how each biosignal contributes to each physiological state and how their information overlaps (Bird et al., 2020).

Recently, in language-vision domains, large-scale multimodal pretraining has demonstrated remarkable generalization and zero-shot capabilities (Huang et al., 2021; Bachmann et al., 2022; Radford et al., 2021), outperforming small-scale models that are trained on specific downstream tasks (Kirkpatrick et al., 2017; Radford et al., 2019). In light of these advancements, we investigate whether similar pretraining can be applied to the biosignal domain. However, performing multimodal pretraining on biosignals is particularly challenging due to the significant distributional shifts between the pretraining and downstream datasets. This challenge can be categorized in two ways: (i) For biosignals, there are substantial distributional **shifts within each modality**, wherein data varies across tasks, subjects, and even recording sessions within subjects due to slight changes in sensor placement and recording conditions (Cheng et al., 2020). Additionally, (ii) multimodal biosignals might encounter strong distributional **shifts across modalities**, meaning that the connection between

*Work completed during internship at Apple. Contact: rliu361@gatech.edu, amoin@apple.com.

different modalities can be altered. These crossmodal domain shifts can arise from unimodal shifts, as a change in a single modality can disrupt its relationship to a different modality. Moreover, multimodal biosignals often face *modality mismatch scenarios*, where modalities may be unavailable at test time, and thus are removed or replaced with new modalities that provide relevant information to the detected physiological response (McKinzie et al., 2023). Addressing these distributional shifts is crucial to effectively leverage multimodal pretraining on biosignals.

In this work, we propose to incorporate frequency information in time series to mitigate distributional shifts and enable multimodal pretraining on biosignals. Frequency-domain analysis is advantageous for biosignals not only due to its invariance to common causes of distributional shifts such as temporal shifts and scaling, but also because the extracted frequency components are characteristic representations for physiological activities. While previous works have shown the effectiveness of using frequency domain information to address generalization issues, they have either relied on encoders from both the time and frequency domains (Zhang et al., 2022b), or complicated sampling and combining modules (Zhou et al., 2022b) to utilize the frequency information. Here, we propose a simple, yet effective, multi-head frequency filter layer with fixed-size Fourier-based operator that directly parameterizes the representation of biosignals in the frequency space. The proposed layer can be easily incorporated into the transformer, giving a *frequency-aware (FA) encoder* that is both expressive and computationally efficient.

Furthermore, to extend the frequency awareness into a multimodal pretraining setting, we couple the FA encoder with a *frequency-maintain (FM) pretraining strategy*. To prevent the statistical consistency within the data from being disrupted by conventional masked autoencoding strategies (Ryali et al., 2023), our method performs masked autoencoding in the latent space to maintain the frequency awareness during reconstruction. Coupled with a channel-independent design (Nie et al., 2022; Liu et al., 2022b), our model presents a pure reconstruction-based multimodal pretraining architecture that can effectively combine and utilize information across modalities, with robustness towards distributional shifts within and across modalities.

To systematically evaluate our proposed approach, we first examine the transferability of our architecture on a publicly available one-to-many transfer learning benchmark (Zhang et al., 2022b). Our architecture achieves state-of-the-art performance, giving an average of $\uparrow 5.5\%$ improvements in classification accuracy over the previous state-of-the-art, showing consistency across datasets of different input lengths, sampling rates, and diverse sources of modalities. Next, we demonstrate that our architecture is robust to a variety of modality mismatch scenarios commonly encountered in real-world cases, showing that our architecture can effectively integrate and leverage information across multiple modalities during pretraining.

We summarize our main contributions as follows:

- We propose `bioFAME`, a frequency-aware masked autoencoder for biosignals comprising: (i) a frequency-aware (FA) transformer encoder that can learn biosignals in a robust and computationally efficient way; (ii) a frequency-maintain (FM) pretraining strategy that retains the frequency awareness during reconstruction.
- By constructing a fixed-size Fourier-based operator in the architecture, `bioFAME` can be adapted to biosignals of varying lengths and frequency components, exhibiting resilience to distributional shifts even when the modalities differ between training and testing.
- `bioFAME` achieves consistently robust performance on a diverse set of transfer experiments, outperforming the previous state-of-the-art by an average improvement of $\uparrow 5.5\%$, demonstrating how utilizing multimodal information at the pretraining stage can benefit the generalization ability of the model.

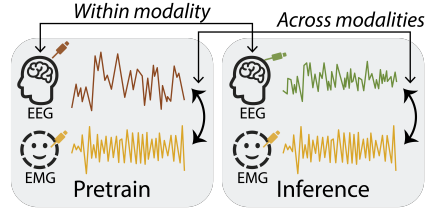


Figure 1: *Illustration.* Distributional shifts within and across modalities between pretrain and inference data in multimodal biosignals.

2 BACKGROUND

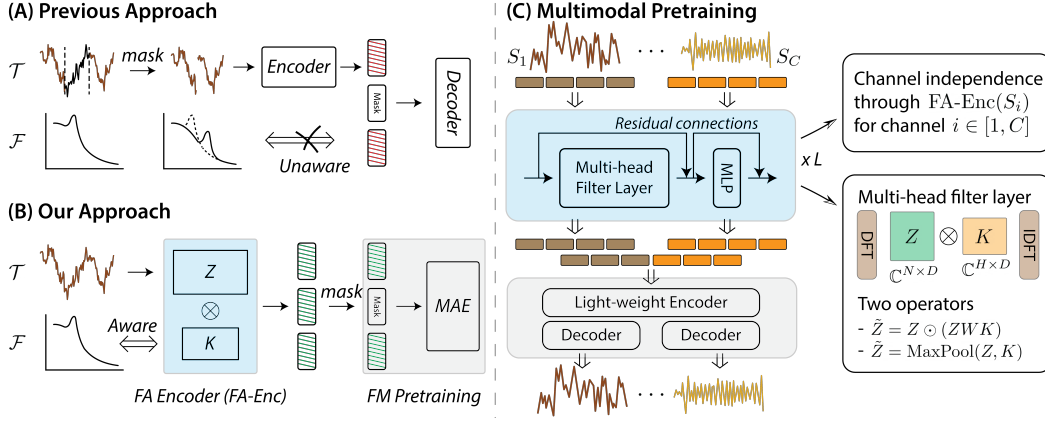
Multimodal Pretraining Methods Pretraining large-scale models that can effectively use multimodal information has gathered a lot of research attention due to its strong capability of generalization (Huang et al., 2021; Liang et al., 2022; Reed et al., 2022; Chai & Wang, 2022). Multimodal pretraining methods can be roughly categorized as (i) those that train separate encoders for each modality, as seen with contrastive methods that design novel objectives to align or fuse representations from different modalities (Li et al., 2021; Radford et al., 2021; Jia et al., 2021), and (ii) those that design one unified architecture for many modalities, with completely shared encoders per-modality or a few layers shared for decoding (Reed et al., 2022; Akbari et al., 2021; Wang et al., 2022). The benefit of using one unified architecture is that we can build a joint representation space that connects different modalities, as well as share weights to reduce additional computational overhead (Bachmann et al., 2022; Lu et al., 2022). Inspired by the latter, our work aims to train a single unified architecture for multimodal biosignals with an effective frequency-awareness design.

Pretraining on Biosignals and Time Series Biosignals are multivariate time series that capture various physiological processes within the human body (Giannakakis et al., 2019; Cheng et al., 2020). While biosignals are crucial for diverse applications such as human-computer interaction, acquiring an ample amount of labeled biosignals is a labor-intensive process that requires the involvement of domain experts (Ericsson et al., 2022). To alleviate the need for labeled data, researchers proposed various self-supervised methods to pretrain the model with large-scale unlabeled datasets. This includes (i) contrastive methods that build latent representation based on similarity across samples of different augmentation (Cheng et al., 2020; Kiyasseh et al., 2021; Zhang et al., 2022b), (ii) reconstruction-based methods that perform either feature reconstruction or data reconstruction (Kostas et al., 2021; Chien et al., 2022), or (iii) a hybrid of both (Dong et al., 2023). While previous works demonstrate that pretraining on large-scale data can benefit downstream task performance, however, most of the existing works only explored unimodal pretraining without investigating how to effectively utilize the multimodal information present at training time. Existing work even shows that pretraining on multimodal information could cause performance degradation due to the large variation across modalities (Zhang et al., 2022b). To the best of our knowledge, this is the first work that explores how to effectively perform multimodal pretraining on biosignals that gives robust performance towards distributional shifts within and across modalities.

3 MOTIVATION OF FREQUENCY-AWARE APPROACHES

Parameterizing representations in the frequency space is shown to be effective in many domains. Frequency-based approaches are particularly effective in solving partial differential equations and modeling long sequences (Li et al., 2020b; Gu et al., 2021; Li et al., 2022; Zhou et al., 2022a), as it can effectively capture long-range dependencies. Frequency-aware approaches are also widely used in computer vision, as it can improve image fidelity and can effectively mix tokens when used in the transformer architecture (Rao et al., 2021; Guibas et al., 2021; Xie et al., 2022; Liu et al., 2022a). The robustness of frequency-based operations can be partially attributed to the connection between Fourier transform and global circular convolution (Zhi et al., 2016; Li et al., 2020a).

Recently, many works suggest that the periodic oscillations and analogous patterns in the frequency space exhibit rich information for electrophysiological signals (Donoghue et al., 2020; Bird et al., 2020; Subha et al., 2010; Demanuele et al., 2007). Thus, several frequency-aware approaches are proposed to study biosignals. For example, Zhang et al. (2022b) used the consistency between time and frequency spaces to guide the learning on biosignals, demonstrating improved transferability and generalizability on downstream tasks. Other works perform cross-domain reconstruction across the time and spectral domains (Zhang et al., 2022a; Yang & Hong, 2022). However, previous works typically rely on a separate encoder in the frequency space to extract frequency information. This reliance introduces additional parameters that not only impose computational overhead but also exacerbate overparameterization issues, thereby impairing model performance especially in scenarios with limited available labels. Our approach diverges from previous works with a simplistic frequency-aware encoder design, as well as an effective frequency-maintaining pretraining strategy.



4 METHOD

Preliminaries: Discrete Fourier Transform (DFT) for Token Mixing DFT is widely used in traditional methods for processing biosignals and images (Pitas, 2000). For a time space representation $\mathbf{x} \in \mathbb{R}^N$ with N elements $x_n, n \in [0, N - 1]$, its corresponding frequency space representation $\mathbf{z} \in \mathbb{C}^N$ with elements z_k is produced by DFT ($\mathcal{F}(\mathbf{x}) = \mathbf{z}$), which can be inverted through the Inverse Discrete Fourier Transform (IDFT) ($\mathcal{F}^{-1}(\mathbf{z}) = \mathbf{x}$) as below:

$$\text{DFT: } z_k = \sum_{n=0}^{N-1} x_n e^{-i(2\pi/N)kn}, \quad \text{IDFT: } x_n = \frac{1}{N} \sum_{k=0}^{N-1} z_k e^{i(2\pi/N)kn}, \quad (1)$$

where i is the imaginary unit. The computational complexity of DFT can be reduced from quadratic to $\mathcal{O}(N \log N)$ when leveraging the fast Fourier transform (FFT) algorithm (Brigham, 1988).

Consider a sequence $X = [\mathbf{x}_1, \dots, \mathbf{x}_N]^T \in \mathbb{R}^{N \times D}$ of N tokens of D -dimensions, transformers aim to learn the interactions across tokens, typically through the self attention operation. Recently, mixing tokens with frequency-based operations through DFT and IDFT is shown to be a computationally efficient alternative (Rao et al., 2021; Guibas et al., 2021), as it considers global-wise information mixing. The token mixing process is theoretically grounded by the Fourier Neural Operators (Li et al., 2020b), which is often implemented in its discrete form (denote as \mathcal{K}) as such:

$$(\mathcal{K}(X))(\mathbf{x}_i) = \mathcal{F}^{-1}(R \cdot \mathcal{F}(X))(\mathbf{x}_i), \forall i \in [1, N] \quad (2)$$

Ideally, R should be the Fourier transform of a periodic function which admits a Fourier series expansion. For the sake of simplicity, it is often implemented as learnable weights of shape $\mathbb{C}^{N \times D}$.

4.1 FREQUENCY-AWARE TRANSFORMER WITH MULTI-HEAD FREQUENCY FILTERS

In this work, we seek to understand two questions: (i) If parameterizing biosignals in the frequency space would provide better empirical performance, as frequency information is shown to be vital for many physiological activities; (ii) How to design a frequency-aware architecture that is transferrable and generalizable across different types of biosignals with varying input lengths and sampling rates. To address those two questions, we propose a multi-head frequency filter layer to build a frequency-aware transformer encoder FA-Enc(\cdot).

Multi-head Frequency Filter Layer We propose to manipulate the frequency representation with a multi-head frequency filters $K \in \mathbb{C}^{H \times D}$, where H is the total number of heads. Given a sequence of tokens $X \in \mathbb{R}^{N \times D}$, we first perform DFT along the sequence dimension to obtain its representation in the frequency space as $Z \in \mathbb{C}^{N \times D}$. To obtain the manipulated features in frequency space $\tilde{Z} \in \mathbb{C}^{N \times D}$, we first compute queries $Q = ZW$, where $W \in \mathbb{R}^{D \times H}$ is a learnable matrix that is used to combine processed information across different filters. The resulting queries are used to re-weight the kernels to obtain \tilde{Z} through the below operations:

$$\tilde{Z} = Z \odot (QK) = Z \odot (ZWK) \quad (3)$$

where \odot is the Hadamard product. We show in Appendix C that the operation is equivalent to a weighted summation between each modulated frequency representation matrix, where the weights are self-generated through the queries. We note that our proposed operation, different from (Rao et al., 2021; Guibas et al., 2021), is applicable on time series with dramatic changes in input lengths and sampling rates, as we use a flexible fixed-sized multi-head filters K that enables the transferability of the model. Intuitively, the querying process has similarity to hypernetworks (David et al., 2016), which generates weights based on data itself to fully exploit the structure of the data.

Having successfully incorporated a fix-sized multi-head filter K into the frequency space, we further explored to build nonlinearity into the operation through an alternative maxpooling operation $\tilde{Z} = \text{MaxPool}(Z, K)$:

$$\tilde{Z}[i, j] = \max_k |Z[i, j]K[k, j]| \quad (4)$$

where the max-pooling is performed based on the absolute value of the complex features.

The resulting modulated frequency representation \tilde{Z} is later recovered in time space through $\tilde{X} = \mathcal{F}^{-1}(\tilde{Z})$ with IDFT (see Figure 2(C)). We denote the whole process as $\text{Freq-L}(\cdot)$, which is computationally efficient, transferrable across different input lengths and sampling rates, and can be easily implemented in a few lines of code.

Add $\text{Freq-L}(\cdot)$ into the Transformer The transformer architecture has revolutionized many domains, including natural language processing (Devlin et al., 2018), computer vision (Dosovitskiy et al., 2020), and recently time series processing (Nie et al., 2022). Following Nie et al. (2022), we first patchify the biosignals by dividing them into chunks, compute representations for each patch, and then feed the resulting patches into a transformer. Specifically, for a signal $\mathbf{s} \in \mathbb{R}^L$ where L is the total length of the sequence, we divide them into sequences of $S = [\mathbf{s}_1, \dots, \mathbf{s}_N]$, where each patch $\mathbf{s}_i \in \mathbb{R}^P$ has a size of P . An initial MLP is used to compute representation $\mathbf{x}_i = \text{MLP}(\mathbf{s}_i) \in \mathbb{R}^D$, and the sequence is later stacked into $X_0 \in \mathbb{R}^{N \times D}$.

We replace the multi-head self-attention with our proposed multi-head frequency filter layer $\text{Freq-L}(\cdot)$ to mix the information across the sequence of tokens, which gives the FA transformer encoder layer as below:

$$X_{\ell+1} = X_{\ell} + \text{Freq-L}(X_{\ell}) + \text{FF}(X_{\ell} + \text{Freq-L}(X_{\ell})), \ell = \{0, \dots, L-1\} \quad (5)$$

where the representation is passed into the proposed $\text{Freq-L}(\cdot)$ layer and projection layers $\text{FF}(\cdot)$ with residual connections, as shown in Figure 2(C).

4.2 FREQUENCY-MAINTAIN PRETRAINING WITH LATENT MASKING AND CHANNEL INDEPENDENCE

Masked Autoencoding in the Latent Space Masked autoencoder (MAE) is a self-supervised pretraining framework, which masks out input patches and predicts the missing patches using the rest present patches. The architecture typically contains an transformer encoder that processes non-masked patches, follows by a decoder, usually a lightweight transformer, that reconstructs the original patches (He et al., 2022).

To preserve the frequency information while being able to perform pretraining based on the masked autoencoding strategy, we perform *masked autoencoding in the latent space*. Specifically, denote our frequency-aware transformer encoder as $\text{FA-Enc}(\cdot)$, full sequence of biosignals S is learnt through $\text{FA-Enc}(\cdot)$ to obtain $X_L = [\mathbf{x}_1^L, \mathbf{x}_2^L, \dots, \mathbf{x}_N^L]$. We sample a random set of patches based on a fixed

masking ratio without replacement, and then process the resulting sequence with a lightweight transformer encoder. We later pad the masked patches with mask tokens, and pass the resulting sequence into a lightweight transformer decoder to reconstruct the original signal, where the i -th reconstructed patch corresponds to s_i . Denote the masked autoencoder as $\text{MAE}(\cdot)$, bioFAME aims to optimize the below objective:

$$\mathcal{L} = \frac{1}{\Omega} \sum_{i \in \Omega} l(s_i, \text{MAE}(\text{FA-Enc}(S))[i]) \quad (6)$$

where i is the token index, Ω is the set of masked tokens, and l is an error term which is set as mean squared error (MSE) in this work. We show in Section 5 that the performance is robust if we remove $\text{MAE}(\cdot)$ and only keep $\text{FA-Enc}(\cdot)$ at test time. We note that this is the first work that finds using the masked autoencoding objective itself, without any contrastive terms, is effective on biosignals (Zhang et al., 2022b).

Channel and Modality Independence Biosignals are multivariate time series that often face channel-wise and modality-wise mismatch at test time. To obtain robust transfer performance, we follow previous works to use *channel-independent design* to model multimodal biosignals (Liu et al., 2022b; Nie et al., 2022).

Given a multi-channel biosignal $[S_1, S_2, \dots, S_C]$, where C denotes the total amount of channels. We perform the channel independence learning such that each S_ξ are passed into $\text{FA-Enc}(\cdot)$ and $\text{MAE}(\cdot)$ as below:

$$\mathcal{L} = \frac{1}{\Omega} \sum_{i \in \Omega} l(s_i, \text{MAE}([\text{FA-Enc}(S_1), \dots, \text{FA-Enc}(S_C)])[i]) \quad (7)$$

where Ω is the union of masked tokens for each channels, which is independently determined based on a fixed masking ratio for each channel, and the parameter weights of the frequency-aware transformer encoder $\text{FA-Enc}(\cdot)$ is shared across channels. By combining the channel independence design into our multimodal masked autoencoding objective, our architecture can process input signals of any channel size and order, making it robust to multimodal distributional shifts when modalities are unavailable at test time.

5 EXPERIMENTS

5.1 TRANSFER EXPERIMENTS ON UNIMODAL TIME SERIES

Datasets We first evaluate the model’s generalization ability by transferring it on a diverse set of unimodal time series downstream tasks, following Zhang et al. (2022b). The transfer experiments include a set of four downstream tasks: Epilepsy (Andrzejak et al., 2001) (EEG measurement of disordered brain activity, sampling rate 174Hz with length 178); SleepEOG (Kemp et al., 2000) (EOG measurement of each sleep stage, sampling rate 100Hz with length 3000); ExpEMG (Goldberger et al., 2000) (EMG measurement of muscular disorders, sampling rate 4000Hz with length 1500); FD-B (Lessmeier et al., 2016) (Electromechanical measurement of motor disorder, sampling rate 64000Hz with length 5120). We performed data pre-processing following the same protocol and data split as in Zhang et al. (2022b), more details are in Appendix B.1. For model pretraining, we used the SleepEDF dataset (Kemp et al., 2000) as in (Eldele et al., 2021; Zhang et al., 2022b), where the single-channel EEG (channel Fpz-Cz) is commonly used for unimodal pretraining. In this work, we also used an additional EEG channel (Pz-Oz) and an additional modality (EOG) from SleepEDF to perform multimodal pretraining with the same train/test split as in Eldele et al. (2021).

Experimental Details For bioFAME , we used a 4-layer encoder, 8-head filter with 64 dimensions. The model was trained using an Adam optimizer with $\beta_1 = 0.9$, $\beta_2 = 0.99$, and a learning rate of 0.001. In contrast to state-of-the-art contrastive architectures (Eldele et al., 2021; Zhang et al., 2022b), we did not apply data augmentation in our architecture as we found there was minimal impact on performance. We performed a grid search based on the validation set to select the model hyperparameters (see Appendix B.2). We repeated experiments with five random seeds for major results, and three random seeds for ablation experiments. To benchmark our method, we selected an extensive set of existing state-of-the-art models, including temporal-spatial methods (Shi et al.,

I. Generalization with modality or task association.								
Models	Epilepsy (EEG)				SleepEOG			
	Accuracy	Precision	Recall	F1	Accuracy	Precision	Recall	F1
TS-SD (Shi et al., 2021)	80.18	76.47	89.52	77.67	48.90	28.59	25.43	23.68
Mixing-up (Wickström et al., 2022)	80.21	40.11	50.00	44.51	-	-	-	-
TS2vec (Yue et al., 2022)	93.95	90.59	90.39	90.45	67.90	58.23	62.15	59.28
CLOCS (Kiyasseh et al., 2021)	95.07	93.01	91.27	92.06	66.86	56.67	58.99	57.34
TS-TCC (Eldele et al., 2021)	92.53	94.51	81.81	86.33	69.65	61.56	61.49	61.16
TF-C (Zhang et al., 2022b)	94.95	94.56	89.08	91.49	69.58	62.04	68.05	64.15
PatchTST (Nie et al., 2022)	95.01	91.66	92.96	92.27	68.00	61.20	68.28	63.26
bioFAME (scratch)	90.41	84.64	86.29	85.33	68.29	60.03	66.10	61.81
bioFAME (unimodal)	95.51	94.02	91.57	92.72	70.03	63.37	68.00	65.05
bioFAME (multimodal)	95.71	93.57	92.82	93.18	71.55	64.80	68.70	66.62
Δ (uni, multi)	$\uparrow 0.20$	$\downarrow 0.45$	$\uparrow 1.25$	$\uparrow 0.46$	$\uparrow 1.52$	$\uparrow 1.43$	$\uparrow 0.70$	$\uparrow 1.57$

II. Generalization without explicit association.								
Models	ExpEMG				FD-B (Electromechanics)			
	Accuracy	Precision	Recall	F1	Accuracy	Precision	Recall	F1
TS-SD (Shi et al., 2021)	46.06	15.45	33.33	21.11	55.66	57.10	60.54	57.03
Mixing-up (Wickström et al., 2022)	30.24	10.99	25.83	15.41	67.89	71.46	76.13	72.73
TS2vec (Yue et al., 2022)	78.54	80.40	67.85	67.66	47.90	43.39	48.42	43.89
CLOCS (Kiyasseh et al., 2021)	69.85	53.06	53.54	51.39	49.27	48.24	58.73	47.46
TS-TCC (Eldele et al., 2021)	78.89	58.51	63.10	59.04	54.99	52.79	63.96	54.18
TF-C (Zhang et al., 2022b)	81.71	72.65	81.59	76.83	69.38	75.59	72.02	74.87
PatchTST (Nie et al., 2022)	92.68	90.87	94.51	92.07	67.03	71.96	75.57	70.09
bioFAME (scratch)	93.17	88.58	94.10	89.97	67.92	76.45	76.51	76.20
bioFAME (unimodal)	98.05	97.07	96.63	96.40	76.58	83.28	82.85	82.63
bioFAME (multimodal)	98.54	96.67	98.95	97.64	78.18	84.99	84.01	83.75
Δ (uni, multi)	$\uparrow 0.49$	$\downarrow 0.40$	$\uparrow 2.32$	$\uparrow 1.24$	$\uparrow 1.60$	$\uparrow 1.71$	$\uparrow 1.16$	$\uparrow 1.12$

Table 1: *Transfer experiments on unimodal time series.* All benchmark models are pretrained on the same single-lead EEG. All variants of our model is based on the same architecture, where **bioFAME** (scratch) is trained from scratch, **bioFAME** (unimodal) follows the same pretraining as baselines, and **bioFAME** (multimodal) is pretrained on the multimodal version of the data. Model standard deviation are in Appendix B.3.

2021; Yue et al., 2022), contrastive methods (Kiyasseh et al., 2021; Eldele et al., 2021), transformers and frequency-aware approaches (Nie et al., 2022; Zhang et al., 2022b). All benchmark models were pretrained on unimodal EEG under the same data split, providing a conclusive list of models for fair comparison.

Pretraining on Unimodality Following previous works Zhang et al. (2022b), we first performed pretraining on a single-channel EEG from the SleepEDF dataset, and then fine-tuning on a small amount of data from the downstream tasks. The performance of our proposed architecture is shown in Table 1. We show that with the same unimodal pretraining setup on single-channel EEG, our model consistently outperforms state-of-the-art benchmarks in most experiments, giving $\uparrow 4.2\%$ improvements in accuracy. These results demonstrate that **bioFAME** is effective in terms of transfer on different tasks, with robustness to domain shifts across tasks, subjects, sampling rate, and sensors. Surprisingly, our architecture, without any pretraining (scratch), also provides robust performance on many datasets, different from previously reported results (Zhang et al., 2022b). This further demonstrates the robustness of our proposed architecture.

Extending Pretraining to Multimodality While the Fpz-Cz EEG channel is shown to be the most informative channel for the pretraining task and typically provides robust prediction performance on its own (Supratak et al., 2017), in this work, we explore whether using additional multimodal information from the same task can further boost the pretraining performance. As shown in Table 1, for **bioFAME**, including multimodal information during pretraining provides better results than unimodal pretraining in general, consistently outperforming unimodal pretraining. Training on multimodal data also improves the model’s stability by giving a lower standard deviation, as shown in Appendix B.3. Note that in previous work (Zhang et al., 2022b), including multimodal information hurt performance rather than helped. This suggests that **bioFAME** can effectively utilize and

FA	FM	Acc.
✗	✗	80.68
✓	✗	84.09
✗	✓	83.53
✓	✓	85.04

Table 2: Average accuracy without FA/FM modules.

Enc-2	Modality	Acc.
✗	Uni	85.04
	Multi	83.92
✓	Uni	85.05
	Multi	85.99

Table 3: The effect of keeping the 2nd encoder for multimodal pretraining.

		Masking ratio		
		0.3	0.5	0.7
Patch	10	83.86	84.05	82.70
	20	84.11	85.04	83.86
	50	80.88	80.84	80.64

Table 4: The effect of different masking ratios and patch sizes.

combine information across modalities, resulting in better performance on downstream tasks. We hypothesize that pretraining on multiple modalities exposes the model to a more diverse range of frequency components, improving the model’s few-shot generalization.

Ablations Experiments on Transferability We performed a set of ablation experiments to understand what makes `bioFAME` robust under the transfer experiments setting. In Table 2, we first studied the effect of the frequency-aware (FA) and frequency-maintain (FM) modules by either replacing the FA module with a self-attention transformer; or by replacing the FM module with a normal masking procedure. We found both approaches, when applied independently, improve the performance of a baseline variant by a significant margin ($\approx 3\%$). Combining both modules gives the best performance, further boosting the effect of each individual component ($\approx 5\%$). We also tested whether it is possible to discard the second encoder at test time, which would indicate whether or not the FA encoder plays a major role in learning. Interestingly, we show that discarding the second encoder at test time gives almost identical performance in the unimodal setting. However, when multimodal information is used for pretraining, discarding the second encoder would give a performance that is lower than the unimodal result, while keeping the second encoder increases the unimodal performance by $\approx 1\%$ instead (see Table 3). We hypothesize that it is beneficial to retain the second encoder at test time under the multimodal setting because it is responsible for merging the information present across the multimodal data. Finally, in Table 9, we investigate how different patch sizes and masking ratios affect the performance of our model. We show that `bioFAME` gives stable performance when the patch size is relatively small, giving robust performance under a range of masking ratios.

5.2 MULTI-MODAL EVALUATIONS AND VISUALIZATIONS

Datasets and Experimental Details After verifying the model’s generalization ability on transfer tasks, we investigated how well the model performs when applied to real-world cases in which multimodal information is available at test time. To understand this, we systematically studied different combinations of the EEG Fpz-Cz, EEG Pz-Oz, EOG, EMG, and the respiration channels of the SleepEDF dataset (Kemp et al., 2000), which are simultaneously recorded. We followed the same train/val/test split as in Eldele et al. (2021) while attaching the multimodal information instead of using only the unimodal information. We utilized the same model setup as in Section 5.1, aside from that we follow Section 4.2 to expand the training and testing under multimodal designs with weight sharing and channel independence. We also implemented two variants of multimodal latent expansion methods as in Appendix C.

Robustness for Modality Mismatch Scenarios We consider two modality mismatch scenarios as shown in Figure 3(A): (i) Modality substitution, where one modality is replaced by another modality; and (ii) Modality dropout, where only a subset of modalities is present at test time. We show the model’s performance with modality substitution in Figure 3(B), where the model is pretrained with { EEG Fpz-Cz; EOG; EMG }. Each of the pretraining modality is replaced with another channel to examine the performance degradation (more details in Appendix B.3). Our model gives better performance than the robust baseline PatchTST (Nie et al., 2022), exhibiting less performance degradation. In terms of modality dropout, we pretrained the model with { EEG Fpz-Cz; EEG Pz-Oz; EOG; EMG }, and we dropped an increasing amount of modalities till there is only one modality left (see Figure 3(C)). We see that `bioFAME` is more resistant to unexpected modalities dropout in comparison to the baseline. Unlike many other baselines that contain spatial layers, `bioFAME` can be applied at test time even when there are unexpected amount of channels while

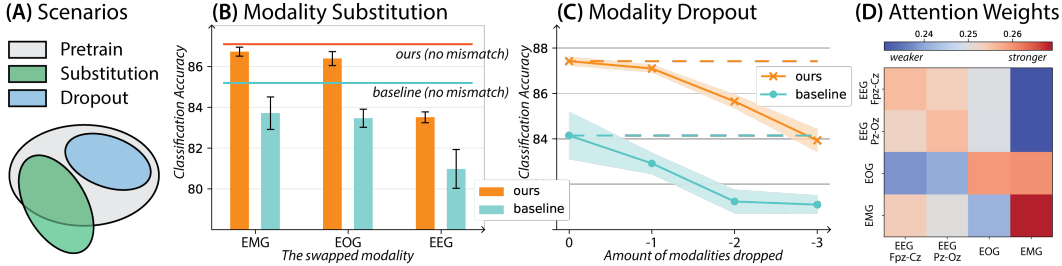


Figure 3: *Multimodal evaluation results.* (A) Two modality mismatch scenarios are considered: Modality substitution and modality dropout. (B) When a modality is swapped with another available one, or (C) when modalities are dropped out at test time, our model gives lower performance degradation when comparing to a robust baseline. (D) By visualizing the attention weights across modalities, we can understand how modalities are associated with each other.

exhibiting resilience towards modality mismatch scenarios. This study further demonstrated that `bioFAME` presents a robust model when used in real-world scenarios.

Visualizing the Connections Across Modalities To understand how the information across different channels affects each other, we visualized the averaged attention matrix to examine the relationship across modalities (more details in Appendix B.3). As shown in Figure 3(D), for each channel (row), the intensity of its attention or connection to the other channels can be visualized by the color (red means stronger connections). Interestingly, we notice that while each channel would rely on its own information the most, they tend to focus on the stronger modalities, which is the EEG Fpz-Cz channel in our case. Moreover, interesting asymmetry is observed for EOG-EMG, as EOG correlates more to the EMG while the opposite does not hold. We hypothesize that this is because facial movement would produce moving artifacts for EOG on the temple, while the opposite connection does not hold. This observation demonstrates that `bioFAME` can be used by researchers to further understand the information overlap across modalities (Bird et al., 2020).

6 CONCLUSION

In this work, we proposed a frequency-aware masked autoencoder that performs pretraining on multimodal biosignals. Our proposed method leverages a frequency-aware encoder with fixed-size Fourier-based operator to extract representation on biosignals, and uses a frequency-maintain pre-training module to perform pretraining. We performed extensive empirical experiments to show that (i) our model achieves state-of-the-art performance on a set of transfer experiments, where the models, both pretrained on unimodality and multimodality, can be adapted to effectively classify time series with varying input lengths, sensors, and sampling rates; and (2) our model demonstrates resilience to within-modal and across-modal distributional shifts, shows robust performance when applied in modality mismatch scenarios that are common in real-world applications.

While our model provides a good balance between utilizing frequency-information and operating on time domain, we note that, just like other frequency-aware architectures (Li et al., 2020b), it remains underexplored how to interpret the specific band and type of frequency information that is taking effect in each downstream task. Exploring how the learned frequency filters can be structured and interpreted will be an exciting line of future research. Also, in our current formulation, we only consider low-density biosignal recording systems due to the lack of publicly available high-dimensional multimodal biosignal datasets. Given the constraints, our architecture relies on the channel-independent design, which is known to suffer from capacity and robustness trade-off (Han et al., 2023). Extending and scaling our approach to high-dimensional sensor inputs is another exciting line of future research for modeling comprehensive human states.

REFERENCES

Hassan Akbari, Liangzhe Yuan, Rui Qian, Wei-Hong Chuang, Shih-Fu Chang, Yin Cui, and Boqing Gong. Vatt: Transformers for multimodal self-supervised learning from raw video, audio and

- text. *Advances in Neural Information Processing Systems*, 34:24206–24221, 2021.
- Ralph G Andrzejak, Klaus Lehnertz, Florian Mormann, Christoph Rieke, Peter David, and Christian E Elger. Indications of nonlinear deterministic and finite-dimensional structures in time series of brain electrical activity: Dependence on recording region and brain state. *Physical Review E*, 64(6):061907, 2001.
- Roman Bachmann, David Mizrahi, Andrei Atanov, and Amir Zamir. Multimaes: Multi-modal multi-task masked autoencoders. In *Computer Vision—ECCV 2022: 17th European Conference, Tel Aviv, Israel, October 23–27, 2022, Proceedings, Part XXXVII*, pp. 348–367. Springer, 2022.
- Jordan J Bird, Jhonatan Kobylarz, Diego R Faria, Anikó Ekárt, and Eduardo P Ribeiro. Cross-domain mlp and cnn transfer learning for biological signal processing: Eeg and emg. *IEEE Access*, 8:54789–54801, 2020.
- E Oran Brigham. *The fast Fourier transform and its applications*. Prentice-Hall, Inc., 1988.
- Filipe Canento, Ana Fred, Hugo Silva, Hugo Gamboa, and André Lourenço. Multimodal biosignal sensor data handling for emotion recognition. In *SENSORS, 2011 IEEE*, pp. 647–650. IEEE, 2011.
- Wenhao Chai and Gaoang Wang. Deep vision multimodal learning: Methodology, benchmark, and trend. *Applied Sciences*, 12(13):6588, 2022.
- Joseph Y Cheng, Hanlin Goh, Kaan Dogrusoz, Oncel Tuzel, and Erdrin Azemi. Subject-aware contrastive learning for biosignals. *arXiv preprint arXiv:2007.04871*, 2020.
- Hsiang-Yun Sherry Chien, Hanlin Goh, Christopher M Sandino, and Joseph Y Cheng. Maeeg: Masked auto-encoder for eeg representation learning. *arXiv preprint arXiv:2211.02625*, 2022.
- Ha David, Dai Andrew, and VL Quoc. Hypernetworks. *arXiv preprint arXiv*, 1609, 2016.
- Virginia R De Sa and Dana H Ballard. Category learning through multimodality sensing. *Neural Computation*, 10(5):1097–1117, 1998.
- Charmaine Demanuele, Christopher J James, and Edmund JS Sonuga-Barke. Distinguishing low frequency oscillations within the 1/f spectral behaviour of electromagnetic brain signals. *Behavioral and Brain Functions*, 3(1):1–14, 2007.
- Jacob Devlin, Ming-Wei Chang, Kenton Lee, and Kristina Toutanova. Bert: Pre-training of deep bidirectional transformers for language understanding. *arXiv preprint arXiv:1810.04805*, 2018.
- Jiaxiang Dong, Haixu Wu, Haoran Zhang, Li Zhang, Jianmin Wang, and Mingsheng Long. Simtm: A simple pre-training framework for masked time-series modeling. *arXiv preprint arXiv:2302.00861*, 2023.
- Thomas Donoghue, Matar Haller, Erik J Peterson, Paroma Varma, Priyadarshini Sebastian, Richard Gao, Torben Noto, Antonio H Lara, Joni D Wallis, Robert T Knight, et al. Parameterizing neural power spectra into periodic and aperiodic components. *Nature neuroscience*, 23(12):1655–1665, 2020.
- Alexey Dosovitskiy, Lucas Beyer, Alexander Kolesnikov, Dirk Weissenborn, Xiaohua Zhai, Thomas Unterthiner, Mostafa Dehghani, Matthias Minderer, Georg Heigold, Sylvain Gelly, et al. An image is worth 16x16 words: Transformers for image recognition at scale. *arXiv preprint arXiv:2010.11929*, 2020.
- Emadeldeen Eldele, Mohamed Ragab, Zhenghua Chen, Min Wu, Chee Keong Kwoh, Xiaoli Li, and Cuntai Guan. Time-series representation learning via temporal and contextual contrasting. *arXiv preprint arXiv:2106.14112*, 2021.
- Linus Ericsson, Henry Gouk, Chen Change Loy, and Timothy M Hospedales. Self-supervised representation learning: Introduction, advances, and challenges. *IEEE Signal Processing Magazine*, 39(3):42–62, 2022.

- Giorgos Giannakakis, Dimitris Grigoriadis, Katerina Giannakaki, Olympia Simantiraki, Alexandros Roniotis, and Manolis Tsiknakis. Review on psychological stress detection using biosignals. *IEEE Transactions on Affective Computing*, 13(1):440–460, 2019.
- Ary L Goldberger, Luis AN Amaral, Leon Glass, Jeffrey M Hausdorff, Plamen Ch Ivanov, Roger G Mark, Joseph E Mietus, George B Moody, Chung-Kang Peng, and H Eugene Stanley. Physiobank, physiotoolkit, and physionet: components of a new research resource for complex physiologic signals. *circulation*, 101(23):e215–e220, 2000.
- Albert Gu, Karan Goel, and Christopher Ré. Efficiently modeling long sequences with structured state spaces. *arXiv preprint arXiv:2111.00396*, 2021.
- John Guibas, Morteza Mardani, Zongyi Li, Andrew Tao, Anima Anandkumar, and Bryan Catanzaro. Adaptive fourier neural operators: Efficient token mixers for transformers. *arXiv preprint arXiv:2111.13587*, 2021.
- Lu Han, Han-Jia Ye, and De-Chuan Zhan. The capacity and robustness trade-off: Revisiting the channel independent strategy for multivariate time series forecasting. *arXiv preprint arXiv:2304.05206*, 2023.
- Kaiming He, Xinlei Chen, Saining Xie, Yanghao Li, Piotr Dollár, and Ross Girshick. Masked autoencoders are scalable vision learners. In *Proceedings of the IEEE/CVF Conference on Computer Vision and Pattern Recognition*, pp. 16000–16009, 2022.
- FN Hooge, TGM Kleinpenning, and Lode KJ Vandamme. Experimental studies on 1/f noise. *Reports on progress in Physics*, 44(5):479, 1981.
- Yu Huang, Chenzhuang Du, Zihui Xue, Xuanyao Chen, Hang Zhao, and Longbo Huang. What makes multi-modal learning better than single (provably). *Advances in Neural Information Processing Systems*, 34:10944–10956, 2021.
- Chao Jia, Yinfei Yang, Ye Xia, Yi-Ting Chen, Zarana Parekh, Hieu Pham, Quoc Le, Yun-Hsuan Sung, Zhen Li, and Tom Duerig. Scaling up visual and vision-language representation learning with noisy text supervision. In *International conference on machine learning*, pp. 4904–4916. PMLR, 2021.
- Bob Kemp, Aeilko H Zwinderman, Bert Tuk, Hilbert AC Kamphuisen, and Josefien JL Obery. Analysis of a sleep-dependent neuronal feedback loop: the slow-wave microcontinuity of the eeg. *IEEE Transactions on Biomedical Engineering*, 47(9):1185–1194, 2000.
- James Kirkpatrick, Razvan Pascanu, Neil Rabinowitz, Joel Veness, Guillaume Desjardins, Andrei A Rusu, Kieran Milan, John Quan, Tiago Ramalho, Agnieszka Grabska-Barwinska, et al. Overcoming catastrophic forgetting in neural networks. *Proceedings of the national academy of sciences*, 114(13):3521–3526, 2017.
- Dani Kiyasseh, Tingting Zhu, and David A Clifton. Clocs: Contrastive learning of cardiac signals across space, time, and patients. In *International Conference on Machine Learning*, pp. 5606–5615. PMLR, 2021.
- Demetres Kostas, Stephane Aroca-Ouellette, and Frank Rudzicz. Bendr: using transformers and a contrastive self-supervised learning task to learn from massive amounts of eeg data. *Frontiers in Human Neuroscience*, 15:653659, 2021.
- Christian Lessmeier, James Kuria Kimotho, Detmar Zimmer, and Walter Sextro. Condition monitoring of bearing damage in electromechanical drive systems by using motor current signals of electric motors: A benchmark data set for data-driven classification. In *PHM Society European Conference*, volume 3, 2016.
- Junnan Li, Ramprasaath Selvaraju, Akhilesh Gotmare, Shafiq Joty, Caiming Xiong, and Steven Chu Hong Hoi. Align before fuse: Vision and language representation learning with momentum distillation. *Advances in neural information processing systems*, 34:9694–9705, 2021.

- Shaohua Li, Kaiping Xue, Bin Zhu, Chenkai Ding, Xindi Gao, David Wei, and Tao Wan. Falcon: A fourier transform based approach for fast and secure convolutional neural network predictions. In *Proceedings of the IEEE/CVF Conference on Computer Vision and Pattern Recognition*, pp. 8705–8714, 2020a.
- Yuhong Li, Tianle Cai, Yi Zhang, Deming Chen, and Debadeepta Dey. What makes convolutional models great on long sequence modeling? *arXiv preprint arXiv:2210.09298*, 2022.
- Zongyi Li, Nikola Kovachki, Kamyar Azizzadenesheli, Burigede Liu, Kaushik Bhattacharya, Andrew Stuart, and Anima Anandkumar. Fourier neural operator for parametric partial differential equations. *arXiv preprint arXiv:2010.08895*, 2020b.
- Paul Pu Liang, Amir Zadeh, and Louis-Philippe Morency. Foundations and recent trends in multimodal machine learning: Principles, challenges, and open questions. *arXiv preprint arXiv:2209.03430*, 2022.
- Hao Liu, Xinghua Jiang, Xin Li, Antai Guo, Deqiang Jiang, and Bo Ren. The devil is in the frequency: Geminated gestalt autoencoder for self-supervised visual pre-training. *arXiv preprint arXiv:2204.08227*, 2022a.
- Ran Liu, Mehdi Azabou, Max Dabagia, Jingyun Xiao, and Eva L Dyer. Seeing the forest and the tree: Building representations of both individual and collective dynamics with transformers. *arXiv preprint arXiv:2206.06131*, 2022b.
- Yisi Liu, Olga Sourina, and Minh Khoa Nguyen. Real-time eeg-based human emotion recognition and visualization. In *2010 international conference on cyberworlds*, pp. 262–269. IEEE, 2010.
- Jiasen Lu, Christopher Clark, Rowan Zellers, Roozbeh Mottaghi, and Aniruddha Kembhavi. Unified-io: A unified model for vision, language, and multi-modal tasks. *arXiv preprint arXiv:2206.08916*, 2022.
- Brandon McKinzie, Vaishal Shankar, Joseph Yitan Cheng, Yinfei Yang, Jonathon Shlens, and Alexander T Toshev. Robustness in multimodal learning under train-test modality mismatch. 2023.
- Yuqi Nie, Nam H Nguyen, Phanwadee Sinthong, and Jayant Kalagnanam. A time series is worth 64 words: Long-term forecasting with transformers. *arXiv preprint arXiv:2211.14730*, 2022.
- Ioannis Pitas. *Digital image processing algorithms and applications*. John Wiley & Sons, 2000.
- Alec Radford, Jeffrey Wu, Rewon Child, David Luan, Dario Amodei, Ilya Sutskever, et al. Language models are unsupervised multitask learners. *OpenAI blog*, 1(8):9, 2019.
- Alec Radford, Jong Wook Kim, Chris Hallacy, Aditya Ramesh, Gabriel Goh, Sandhini Agarwal, Girish Sastry, Amanda Askell, Pamela Mishkin, Jack Clark, et al. Learning transferable visual models from natural language supervision. In *International conference on machine learning*, pp. 8748–8763. PMLR, 2021.
- Yongming Rao, Wenliang Zhao, Zheng Zhu, Jiwen Lu, and Jie Zhou. Global filter networks for image classification. *Advances in neural information processing systems*, 34:980–993, 2021.
- Scott Reed, Konrad Zolna, Emilio Parisotto, Sergio Gomez Colmenarejo, Alexander Novikov, Gabriel Barth-Maron, Mai Gimenez, Yury Sulsky, Jackie Kay, Jost Tobias Springenberg, et al. A generalist agent. *arXiv preprint arXiv:2205.06175*, 2022.
- Chaitanya Ryali, Yuan-Ting Hu, Daniel Bolya, Chen Wei, Haoqi Fan, Po-Yao Huang, Vaibhav Aggarwal, Arkabandhu Chowdhury, Omid Poursaeed, Judy Hoffman, et al. Hiera: A hierarchical vision transformer without the bells-and-whistles. *arXiv preprint arXiv:2306.00989*, 2023.
- Pengxiang Shi, Wenwen Ye, and Zheng Qin. Self-supervised pre-training for time series classification. In *2021 International Joint Conference on Neural Networks (IJCNN)*, pp. 1–8. IEEE, 2021.

- Linda Smith and Michael Gasser. The development of embodied cognition: Six lessons from babies. *Artificial life*, 11(1-2):13–29, 2005.
- D Puthankattil Subha, Paul K Joseph, Rajendra Acharya U, and Choo Min Lim. Eeg signal analysis: a survey. *Journal of medical systems*, 34:195–212, 2010.
- Akara Supratak, Hao Dong, Chao Wu, and Yike Guo. Deepsleepnet: A model for automatic sleep stage scoring based on raw single-channel eeg. *IEEE Transactions on Neural Systems and Rehabilitation Engineering*, 25(11):1998–2008, 2017.
- Peng Wang, An Yang, Rui Men, Junyang Lin, Shuai Bai, Zhikang Li, Jianxin Ma, Chang Zhou, Jingren Zhou, and Hongxia Yang. Ofa: Unifying architectures, tasks, and modalities through a simple sequence-to-sequence learning framework. In *International Conference on Machine Learning*, pp. 23318–23340. PMLR, 2022.
- Kristoffer Wickstrøm, Michael Kampffmeyer, Karl Øyvind Mikalsen, and Robert Jenssen. Mixing up contrastive learning: Self-supervised representation learning for time series. *Pattern Recognition Letters*, 155:54–61, 2022.
- Jiahao Xie, Wei Li, Xiaohang Zhan, Ziwei Liu, Yew Soon Ong, and Chen Change Loy. Masked frequency modeling for self-supervised visual pre-training. *arXiv preprint arXiv:2206.07706*, 2022.
- Ling Yang and Shenda Hong. Unsupervised time-series representation learning with iterative bilinear temporal-spectral fusion. In *International Conference on Machine Learning*, pp. 25038–25054. PMLR, 2022.
- Zhihan Yue, Yujing Wang, Juanyong Duan, Tianmeng Yang, Congrui Huang, Yunhai Tong, and Bixiong Xu. Ts2vec: Towards universal representation of time series. In *Proceedings of the AAAI Conference on Artificial Intelligence*, volume 36, pp. 8980–8987, 2022.
- Wenrui Zhang, Ling Yang, Shijia Geng, and Shenda Hong. Cross reconstruction transformer for self-supervised time series representation learning. *arXiv preprint arXiv:2205.09928*, 2022a.
- Xiang Zhang, Ziyuan Zhao, Theodoros Tsiligkaridis, and Marinka Zitnik. Self-supervised contrastive pre-training for time series via time-frequency consistency. *arXiv preprint arXiv:2206.08496*, 2022b.
- Xiyang Zhi, Deyun Wei, and Wei Zhang. A generalized convolution theorem for the special affine fourier transform and its application to filtering. *Optik*, 127(5):2613–2616, 2016.
- Tian Zhou, Ziqing Ma, Qingsong Wen, Liang Sun, Tao Yao, Wotao Yin, Rong Jin, et al. Film: Frequency improved legendre memory model for long-term time series forecasting. *Advances in Neural Information Processing Systems*, 35:12677–12690, 2022a.
- Tian Zhou, Ziqing Ma, Qingsong Wen, Xue Wang, Liang Sun, and Rong Jin. Fedformer: Frequency enhanced decomposed transformer for long-term series forecasting. In *International Conference on Machine Learning*, pp. 27268–27286. PMLR, 2022b.

APPENDIX

A ADDITIONAL RESULTS

A.1 DATA EFFICIENCY AND OPERATOR SELECTION

Data efficiency To understand the behavior of `bioFAME` within the context of limited data availability, we conducted experiments aimed at gauging the architecture’s efficacy when exposed to a reduced amount of labeled data during the finetuning phase. We show the performance of `bioFAME` in Figure 4(A), both with and without pretraining, where the performance of `bioFAME` is plotted when the amount of labeled data for downstream training varies from 5% to 100%. Notably, in contrast to previous work (Eldele et al., 2021), wherein architecture performance substantially deteriorated with decreased labeled data, `bioFAME` achieves stable results with relatively low decay of performance even without pretraining. Furthermore, the pretrained version of `bioFAME` gives consistently robust performance across the spectrum of labeled data proportions. We hypothesize that modeling biosignals using the Fourier function group with frequency operators improves the data efficiency of models.

Ablations on the two operators To validate the effectiveness of the Maxpool operator and the Query operator as described in Section 4.1, we examine the model’s performance by varying the number of filters. We find that the Maxpool operator gives more stable results, while the Query operator seems to scale better to larger amount of filters.

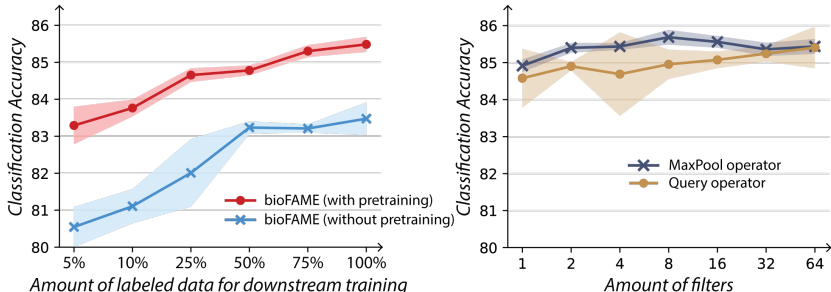


Figure 4: (A) We examine the performance of `bioFAME` under low-data regime with and without pretraining. (B) We examine how the MaxPool operator and Query operator would perform with different amounts of filters.

A.2 MODEL VARIATION

For the transfer experiments result as shown in Table 1, we provide the standard variation across five different random seeds in Table 5. Note that the entire training process, both the pretraining and the finetuning stages, is repeated to obtain the standard variation for fair evaluation. We notice that multimodal pretraining typically gives a lower standard deviation than that of unimodal pretraining, demonstrating that multimodal pretraining might help with the stability of the model, as it is exposed to a variety of frequency components.

A.3 ABLATION RESULTS BREAKDOWN

In Table 6, we report the breakdown details for the average accuracy presented in Table 2 and Table 3. Our model provides robust performance across different downstream tasks consistently.

B EXPERIMENTAL DETAILS

B.1 DATASETS DETAILS

We provide additional details about the datasets we used as follows.

Models	Epilepsy (EEG)				SleepEOG			
	Accuracy	Precision	Recall	F1	Accuracy	Precision	Recall	F1
bioFAME (scratch)	1.17	2.42	0.72	1.26	0.77	0.67	0.50	0.76
bioFAME (unimodal)	0.35	0.37	1.17	0.65	1.39	1.23	0.91	0.61
bioFAME (multimodal)	0.17	0.51	0.21	0.24	0.90	0.79	0.89	0.88
Δ (uni, multi)	$\downarrow 0.18$	$\uparrow 0.14$	$\downarrow 0.96$	$\downarrow 0.41$	$\downarrow 0.49$	$\downarrow 0.44$	$\downarrow 0.02$	$\uparrow 0.27$

Models	ExpEMG				FD-B (Electromechanics)			
	Accuracy	Precision	Recall	F1	Accuracy	Precision	Recall	F1
bioFAME (scratch)	2.67	3.13	2.25	3.15	1.63	1.33	1.20	1.09
bioFAME (unimodal)	2.04	2.80	5.64	4.15	2.74	1.75	2.01	2.14
bioFAME (multimodal)	1.34	3.04	0.96	2.15	1.94	1.53	1.44	1.66
Δ (uni, multi)	$\downarrow 0.70$	$\uparrow 0.24$	$\downarrow 4.68$	$\downarrow 2.00$	$\downarrow 0.80$	$\downarrow 0.22$	$\downarrow 0.57$	$\downarrow 0.48$

Table 5: The standard deviation of `bioFAME` for each transfer experiment.

	Ablations	Epilepsy	SleepEOG	ExpEMG	FD-B
Table 2	FA \times FM \times	95.01	68.00	92.68	67.03
	FA \checkmark FM \times	95.03	69.73	98.37	73.23
	FA \times FM \checkmark	94.81	68.41	95.94	74.97
	FA \checkmark FM \checkmark	95.51	70.03	98.05	76.58
Table 3	Uni, Enc-2 \times	95.91	70.17	95.94	78.16
	Multi, Enc-2 \times	95.26	71.04	96.10	73.28
	Uni, Enc-2 \checkmark	95.51	70.03	98.05	76.58
	Multi, Enc-2 \checkmark	95.71	71.55	98.54	78.18

Table 6: Breakdown of model performance on different downstream tasks.

SleepEDF The entire SleepEDF dataset contains 197 recordings of whole-night sleep, where the dataset contains 2-lead EEG, EOG, chin EMG, respiration rates, body temperature, and event markers. We selected a subset of the dataset from the Cassette Study following Eldele et al. (2021), where the dataset is used to study the age effects on sleep in healthy Caucasians. We further followed the same train/validate/test split, and removed data with incomplete modalities. The recordings are segmented into 30 seconds of sleep for training, where each sample is associated with one of the five sleeping patterns/stages: Wake (W), Non-rapid eye movement (N1, N2, N3), and Rapid Eye Movement (REM).

Epilepsy The Epilepsy dataset contains single-lead EEG measurements from 500 subjects, where the brain activities are recorded for subjects with seizure. The classification task is based on if the subject is having a seizure episode during the recording session.

SleepEOG The SleepEOG dataset is a subset of the SleepEDF dataset under the Telemetry Study, where subjects are reported to have mild difficulty falling asleep, and thus intake either temazepam or placebo before sleep. The EOG channel is used for classification.

ExpEMG The ExpEMG dataset consists of single-channel EMG recordings from the tibialis anterior muscle of three healthy volunteers, where they (1) do not have history of neuromuscular disease; (2) suffer from chronic low back pain and neuropathy; and (3) suffer from myopathy due to longstanding history of polymyositis. The classification task aims to classify different conditions (subjects).

FD-B The FD-B dataset is an electromechanical dataset, where the motor currents and vibration signals of healthy or damaged motors are recorded. The classification task aims to detect different faulty conditions of the motors based on their behavior. We found that the motor movement follows a similar frequency assumption as biosignals (Hooge et al., 1981), and thus used this electromechanical dataset to provide additional validation of the transfer performance of our model.

Datasets	Train	Validate	Test	Sampling rate	Length
Epilepsy	60	20	11420	174	178
SleepEOG	1000	1000	37244	100	3000
ExpEMG	122	41	41	4000	1500
FD-B	60	21	13559	64000	5120

Table 7: Dataset split details for different downstream tasks.

We performed the transfer experiments based on the same settings as in Zhang et al. (2022b), where we used the train/validate/test split as shown in Table 7 for downstream fine-tuning to demonstrate the few-shot generalization ability of the model across different signals.

B.2 MULTIMODAL SETUP DETAILS

The multimodal experiments are designed to tackle the challenge presented by modality mismatch scenarios, where discrepancies in biosignal recording setups between training and testing phases lead to distributional shifts. Due to the scarcity of comprehensive multimodal datasets encompassing simultaneous recording of diverse modalities of biosignals, we exclusively used the SleepEDF dataset due to its modality coverage.

We first empirically assessed the representation quality of each individual channel. Similar to the findings in Supratak et al. (2017), we found that the representation capacity of different channels follows EEG Fpz-Cz > EEG Pz-Oz > EOG > EMG > resp. Building upon these insights, we performed the modality substitution and modality dropout experiments following the below pretraining and finetuning setup.

Training modalities	Testing modalities
EEG Fpz-Cz; EOG; EMG	EEG Fpz-Cz; EOG; resp EEG Fpz-Cz; EEG Pz-Oz; EMG EEG Pz-Oz; EOG; EMG

Table 8: Modality setup for modality substitution experiments.

Training modalities	Testing modalities
EEG Fpz-Cz; EEG Pz-Oz; EOG; EMG	EEG Fpz-Cz; EEG Pz-Oz; EOG EEG Fpz-Cz; EEG Pz-Oz EEG Fpz-Cz

Table 9: Modality setup for modality dropout experiments.

B.3 HYPERPARAMETER SEARCHING DETAILS

For transfer experiments, we performed hyperparameter searching based on results on the Epilepsy dataset, and used the same parameter setting across all transfer experiments. Specifically, we performed a grid search of learning rate of [0.0001, 0.001, 0.01], transformer depth of [2, 3, 4, 5, 6], latent dimensionality of [16, 32, 64, 128], dropout rate of [0.2, 0.3, 0.4], operator type, and filter amount correspondingly. For multimodal experiments, we evaluate the model’s performance on the pretraining dataset, and performed the evaluation on the finetuning modalities using the best model used in pretraining. For the multimodal experiments, we performed a smaller scale grid search for the latent dimensionality and transformer depth.

C METHODOLOGY DETAILS

C.1 ADDITIONAL EXPLANATION OF MOTIVATION

Biosignals are often analyzed in their frequency space, where they are either studied through predefined frequency regions or through aperiodic components which typically form a 1/f-like distribution (Donoghue et al., 2020). The significance of frequency information is well-documented due to its intricate interrelation with various facets of learning, aging, as well as diseases such as ADHD or

seizures. Correspondingly, modeling approaches that rely on the manual extraction and preprocessing of spectrogram features have demonstrated robust empirical performance (Supratak et al., 2017). Building upon these insights, we hypothesize that modeling biosignals employing function groups within the frequency domain could benefit the learning process by enhancing model adaptability and data efficiency. We note that this hypothesis might be violated if the frequency components carry limited information in other formats of time series datasets.

C.2 INTUITION FOR THE MULTI-HEAD FREQUENCY FILTER LAYER

We provide additional intuition for the design of our multi-head frequency filter layer by breaking down the computation for each individual filter. For each k -th filter $K[k]$ inside $K \in \mathbb{C}^{H \times D}$, given latent representation $Z = [z_1, z_2, \dots, z_N]^T \in \mathbb{C}^{N \times D}$, we compute $Z^{(k)} = [z_1 \odot K[k], z_2 \odot K[k], \dots, z_N \odot K[k]]^T$, where \odot represents the Hadamard product between each representation and the learnable filter weights. In order to learn the combination between different filters, we define weights w that compute $\tilde{Z} = \sum_{k=1}^H w_k Z^{(k)}$.

To increase the expressiveness of the filtering operation, instead of learning a linear combination of different filters, we borrow intuition from the computation of self-attention to compute the queries for the kernel weights w through $w = zW$, where $W \in \mathbb{C}^{D \times H}$. Thus, we have:

$$\begin{aligned} \tilde{Z}[i, j] &= \sum_{k=1}^H \left(\sum_{j=1}^D Z[i, j] W[j, k] \right) Z[i, j] K[k, j] \\ &= Z[i, j] \sum_{k=1}^H \left(\sum_{j=1}^D Z[i, j] W[j, k] \right) K[k, j] \end{aligned} \quad (8)$$

which gives $\tilde{Z} = Z \odot (ZWK)$. In our implementation, we use the real values of latents to learn the weights of the combiner though $w = z_{\text{real}}W$. Similarly, based on the same intuition of combining filtered matrices, we have the max pooling operation.

C.3 MODEL VARIANTS FOR COMBINING MULTIMODAL REPRESENTATIONS

In transfer experiments, we use the average of tokens to extract the final representations for the downstream classification. However, when having multimodal information, fixing the dimensionality of the latent representation when many modalities are present might narrow down the information from each modality, which might cause information loss. Thus, in multimodal experiments, we first average the representations from each individual modality, and then concat the representations across modalities before performing the downstream classification.